JOURNAL OF Materials CHEMISTRY

Electronic structures and instabilities of ZrNCl and HfNCl: implications for superconductivity in the doped compounds

Claudia Felser and Ram Seshadri

Institut für Anorganische Chemie und Analytische Chemie, Johannes Gutenberg-Universität, Mainz, Becher Weg 24, D-55099, Mainz, Germany

Received 20th October 1998, Accepted 9th November 1998

Amongst the many rules of thumb that prevail in the search for new superconductors is a belief that square nets of metal atoms are crucial to the achievement of high transition temperatures. The recent finding of superconductivity below 26 K in some intercalated β-HfNCl phases suggests that high transition temperatures might be achievable in compounds with triangular or graphite-like nets as well. Here we present key features of high level *ab initio* band structure calculations on the insulating ZrNCl and HfNCl parent compounds. Electron doping through intercalation has been modeled within a rigid-band framework. Features in the energy isosurfaces of the 'doped' compounds are examined for nesting instabilities of the kind that have been implicated in the superconducting properties of high-T_c compounds with square nets. Despite very different electron counts, bonding patterns and atom topologies, it would seem that certain important aspects of the Fermi surfaces of the superconducting Zr(Hf)NCl phases are in many respects very similar to the Fermi surfaces of the cuprate high-T_c superconductors.

In the absence of hard theory, the chemist seeking to prepare new superconductors through rational synthesis often requires the use of a few rules of thumb. In recent years, there has risen the appreciation that certain types of electronic instabilities in the Fermi surfaces of compounds (as can be calculated through high-level *ab initio* band structure methods) can be indicative of superconducting ground states. In the copper–oxide high-T_c superconductors, the important common thread is the presence of CuO_2 sheets with the atoms arranged in a chess board-like manner. The electronic structure of these square nets is characterised by van Hove singularities in the densities of state (DOS) near the Fermi energy E_F. The link between van Hove singularities (vHS) and superconductivity was first proposed for the A15 superconductors[1] and later extended to the high-T_c cuprates.[2,3] The possible role that the vHS plays in systems other than superconductors[4–6] has been examined recently, as have extensions of the vHS scenario from compounds with square nets to compounds with close-packed sheets of metals atoms (such as superconducting $LiZrSe_2$)[7] and with graphite-like sheets of alternating metal and non-metal atoms (such as valence-unstable EuPdP).[4] Indeed superconductivity has been predicted through analogy in suitably doped SrPdP, where replacement of valence-unstable Eu by Sr is expected to result in superconducting rather than inhomogeneous mixed-valent ground states.[4] Through an examination of the electronic structures of certain $m=2$ Ruddlesden–Popper manganites (displaying giant magnetoresistance) and cuprates (displaying superconductivity) we have earlier pointed out that similar electronic instabilities might be important in the phenomena displayed by these compounds; the different phenomena arising from the different electron counts.[6]

Compounds with triangular nets (close-packed sheets) of atoms such as $LiNbO_2$[8] have so far been considered as having electronic structures quite unlike the high-T_c cuprates,[9] and indeed, there is a general belief that only in compounds with square nets of atoms does one simultaneously find the combinations of highly disperse and highly localized bands in the vicinity of the Fermi energy that are believed to be necessary for high superconducting transition temperatures. Our examination of the band structures and Fermi surfaces (FS) of some hexagonal compounds such as $LiZrSe_2$[7] and some ABO_2 delafossites[10] has encouraged us in the belief that the kind of instabilities (typically an X-shaped nesting) associated with certain combinations of flat and disperse bands can also be found in compounds that do not possess square nets.

We must emphasize that the so-called van Hove Scenario for superconductivity should not be trivially interpreted as a local peak in the DOS at the Fermi energy. Indeed, it is our finding that the DOS is often only a poor indicator of the right kind of van Hove singularities. Sometimes, even a careful analysis of the band structure (which we recollect is only a projection of the electronic structure) is insufficient for this purpose. It is our view that searching for suitable vHS usually means examining three-dimensional energy isosurfaces that are decorated with the band dispersions.

Recently, Yamanaka *et al.*[11,12] have demonstrated that intercalation of rhombohedral β-ZrNCl with Li yields compounds with superconducting T_c values near 14 K. In suitably intercalated β-HfNCl, T_c values are as high as 26 K.[13] This puts these compounds in the unique class occupied by the layered cuprates, the perovskite bismuth oxides and the doped fullerides. The high transition temperatures have encouraged us to examine the electronic structure of the undoped parent compounds ZrNCl and HfNCl through band structure calculations. We present the results here. We have already communicated some features of the electronic structure of β-ZrNCl including some so-called 'fatbands'[14] as well as comparisons with other compounds possessing hexagonal or triangular nets of metal atoms.[15] Recently, Woodward and Vogt have examined the electronic structures of β-ZrNCl and some related compounds at the extended Hückel level.[16]

Structures and calculation details

Juza and Friedrichsen[17] who first prepared β-ZrNCl suggested from single crystal X-ray measurements on *faulted* crystals that the structure involves double layers following the stacking sequence –Cl–Zr–N–N–Zr–Cl– along the *c* axis. In the structure they propose, the stacking corresponding to these atoms is ABCABC with one Zr on top of another. This structure is characterized by a very short Zr–Zr contact of about 2.7 Å along the *c* axis. Rather than use this structure, we prefer the recent single crystal X-ray determination of the structure of $NaZr_2N_2ClS$ (isoelectronic with ZrNCl) by Lissner and Schleid[18] as a model for ZrNCl. The ordering of atoms within

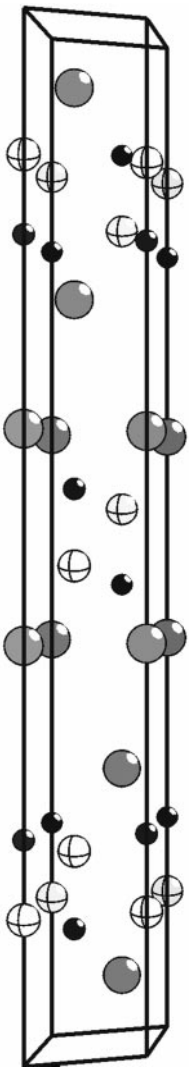

Fig. 1 Structure of rhombohedral β-ZrNCl following the determination by Lissner and Schleid of the structure of $NaZr_2N_2ClS$.[18] The black spheres are Zr, hatched white spheres are N and grey spheres are Cl. Relevant data are: space group $R\bar{3}m$ (no. 166), $a=3.606$, $c=27.69$ Å. The Zr are in (0,0,0.2138), N in (0,0,0.1384) and Cl in (0,0,0.3972). Hexagonal (1T) ZrNCl derived from the above data: space group $P\bar{3}m1$ (no. 164), $a=3.606$, $c=9.23$ Å. The Zr are in (1/3,2/3,0.6414), N in (−1/3,-2/3,0.5850) and Cl in (0,0,0.1916).

the double layer along the *c* axis in the structure of Lissner and Schleid is the same as in the model of Juza and Friedrichsen. The difference is that the stacking now follows the order ABCBCA. As a result the Zr have an anion coordination of 1(N)+3(N)+3(Cl) corresponding to a capped trigonal antiprism and instead of a short Zr–Zr contact, there is a short Zr–N contact along *c*. All the bond distances in this model (shown in Fig. 1 with the structural parameters in the caption) are reasonable. Considering the highly layered nature of the structure and reports that there is considerable polytypism and faulting, the crystallography of these phases is certainly complex and the doubts cast on the original structure determination point to the need for studies on the *undoped* samples perhaps by powder neutron diffraction. The crystallography of the Li-intercalated samples further involves solvation of the Li cations, and precise determinations of the structures of superconducting compositions are likely to remain a challenge.

Relevant details of the methods used here *viz.* scalar-relativistic tight-binding linear muffin tin orbital (LMTO) band structure calculation and illustrative applications can be found elsewhere.[14,19] The calculations were performed within the atomic sphere approximation using version 47 of the LMTO program package.[20] The central Brillouin zone is as described in the standard reference.[21] 1664 and 5657 irreducible *k* points were used in the calculations on the hexagonal and rhombohedral compounds respectively. To visualize atom specific bonding, we use crystal orbital Hamiltonian populations (COHPs)[22] to demarcate as a function of the energy, bonding, non-bonding and antibonding states. COHPs are rather like crystal orbital overlap populations (COOPs)[23] made current by Hoffmann and coworkers, with the difference that the opposite sign conventions are used to demarcate bonding and antibonding states—where a positive COHP implies bonding, *etc.*

Results

Fig. 2 displays the total and partial densities of state (DOS) of hexagonal and rhombohedral ZrNCl. As expected for a rather polar d^0 system, β-ZrNCl is an insulator with a calculated band gap of about 2.1 eV. There is very little difference in the electronic structures on going from the primitive hexagonal 1T polytype to the rhombohedral 3R polytype as demonstrated in this figure. Considering anion states we observe that the Cl and N have approximately the same bandwidth, though both at the top and the bottom of the valence band N states seem to dominate. While the Cl states possess a single envelope, the envelope of the N states seems split in two, with the separate peaks centered around −4 and −1 eV. The conduction band is dominated by empty Zr d states. There is thus nearly complete charge transfer from the cation to the anion, with little or no back transfer of electrons. This is in keeping with the results of Woodward and Vogt.[16] Yamanaka and coworkers[13] have suggested that the title compounds are similar to the superconducting compound $Y_2C_2Br_2$, but we find some significant differences. $Y_2C_2Br_2$ displays back-transfer of electrons from C π* to Y d.[24] It also has very short

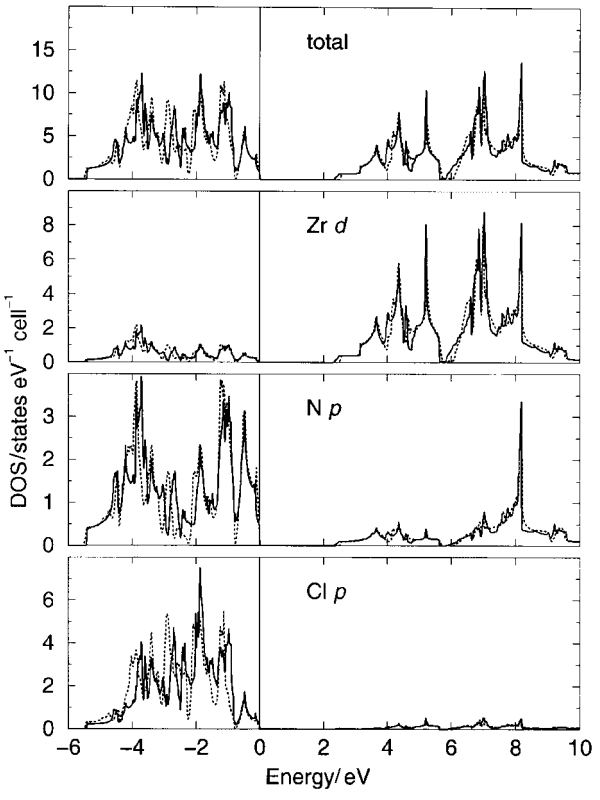

Fig. 2 Total and partial densities of state of hexagonal (continuous lines) and rhombohedral (dotted lines) ZrNCl as obtained from LMTO calculations.

C–C contacts unlike ZrNCl where there are no short anion–anion contacts.

A remarkable feature in the DOS of ZrNCl is the presence of sharp features suggesting that some of the bonding is local or 'molecular'. These sharp features are also related to the highly layered nature of the structure. If we assume rigid band behaviour for the Li intercalated compounds, the states at the Fermi energy in the superconductor should derive mainly from Zr d orbitals. This is unlike $Y_2C_2Br_2$ where both cation and anion states are found at the Fermi energy. In fact the nature of the Li intercalation and of the important orbitals suggests that a comparison with the electronic structure of Li_xZrSe_2 might be more useful.[7] This comparison extends to the particular behaviour of T_c with changing Li content, suggesting the role of clustering and percolation of the intercalated cations.[7,13]

Fig. 3 displays the total and partial DOS of hexagonal HfNCl. The discussion of the DOS of ZrNCl holds very well for this compound, the difference being a slightly larger band gap of about 2.5 eV. Once again, the valence band is dominated by N states and the conduction band by Hf states.

An analysis of the crystal orbital Hamiltonian populations (COHPs) allows us to further understand the nature of the states. In Fig. 4 we show the COHPs due to the different interactions, Zr–N, Zr–Zr, Zr–Cl and N–N, in 1T-ZrNCl. We observe that the bonding is clearly dominated by Zr-N interactions. The continuous line in the top panel of this figure corresponds to the COHP of the interaction between Zr and the capping N and the dotted line, the COHP of Zr and the other three N atoms. As expected, the interaction is bonding below the E_F and starts to become antibonding in the range of the Zr d states. At the bottom of the conduction band, the Zr–N interaction does not play an important role. The bulk of the antibonding interactions start only at energies above 6 eV, corresponding to metal orbitals that are not involved in the metal–metal bonding. Considering the Zr–Zr COHP, we observe that there are bonding interactions within the metal atom sheet between 3 and 4 eV. This interaction becomes

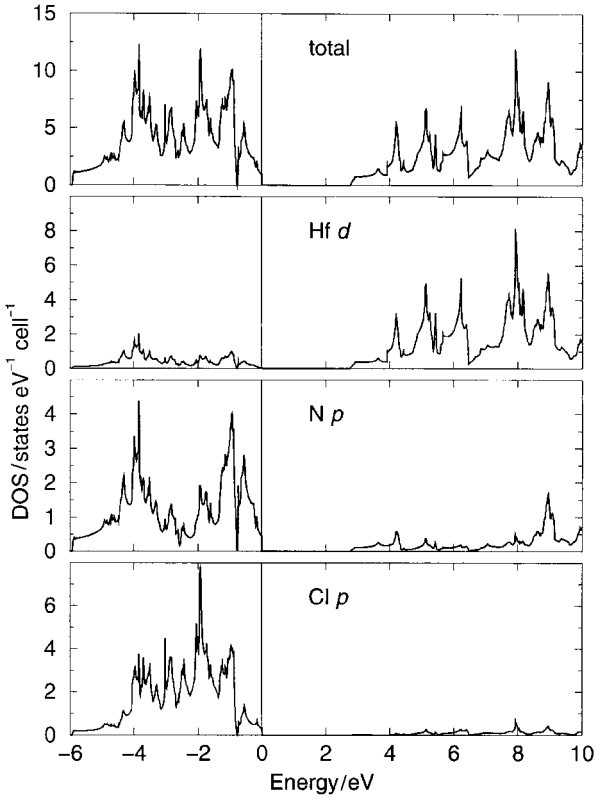

Fig. 3 Total and partial densities of state of hexagonal HfNCl as obtained from LMTO calculations.

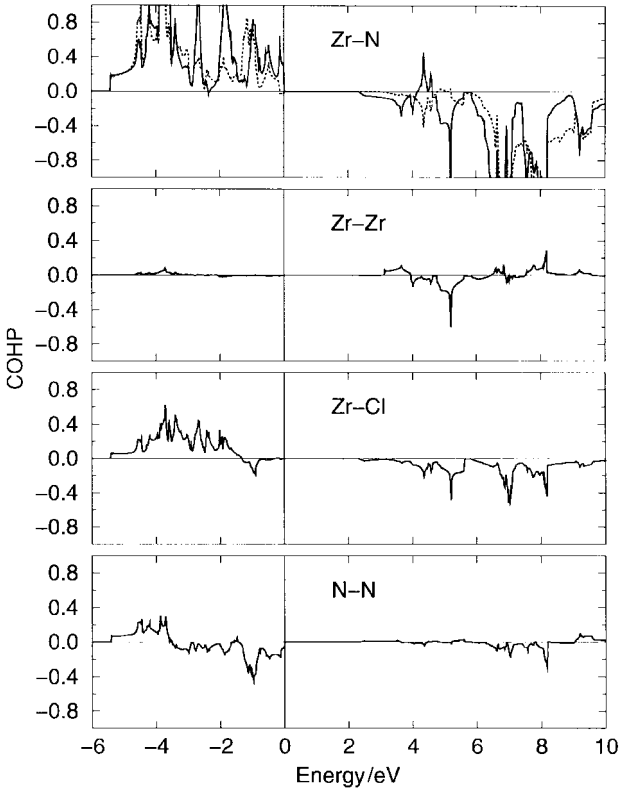

Fig. 4 Crystal orbital Hamiltonian populations (COHPs) per pairwise interaction in hexagonal ZrNCl showing the Zr–N, Zr–Zr, Zr–Cl and N–N interactions. Positive COHPs are bonding and negative COHPs are antibonding. In the top panel, the continuous line corresponds to the short Zr–N distance (with the capping N along the *c* axis) and the dotted line, the interaction with the other three N.

nearly non-bonding and then antibonding following the scheme given by Hughbanks and coworkers for bonding in close-packed sheets of metal atoms in compounds such as MoS_2.[25] Despite the overall bonding being dominated by Zr–N interactions, the Zr–Zr interactions would be as important as the antibonding Zr–N (with the capping N) interactions when the compound is doped with electrons since the Fermi level in the doped compounds would cross these states.

The Zr–Cl interactions are seen to be much smaller than the other metal–non-metal interactions. There are no contributions to the states at the Fermi energies of the doped compounds from this interaction. The N–N interactions are seen to be very much smaller than what one expects for a true bonding interaction in keeping with the rather large N–N distances. They are bonding at the bottom of the valence band and antibonding at the top. This is what splits the envelope of the N DOS into two. The bonding and antibonding N–N interactions cancel each other lending credence to the formulation of N as N^{3-} (a closed shell).

Fig. 5 compares the band structures of hexagonal ZrNCl, rhombohedral ZrNCl and hexagonal HfNCl. The labeling of the Brillouin zone (BZ) corresponds to standard notation.[21] We discuss only the bands around the E_F because we wish to focus on the instabilities possibly associated with the superconducting properties of the doped compounds. Comparisons of the band structures are simplified through recognizing that the points L–A–Γ–M in the hexagonal band structures correspond to the points L–Z–Γ–F in the rhombohedral band structure. The K and H points in the hexagonal band structure are no longer special points in the rhombohedral band structure and this is why we do not see the correct band gap in the rhombohedral compound. Because the rhombohedral band structure has fewer special points we focus our discussion on the hexagonal band structures.

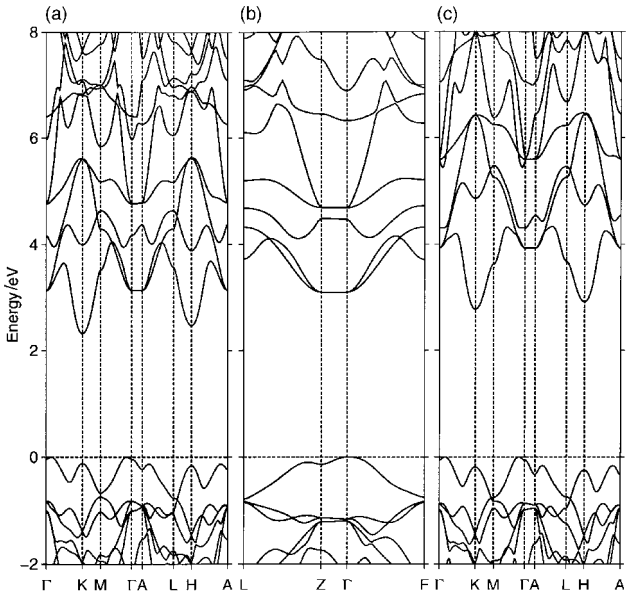

Fig. 5 Band structures of (a) hexagonal and (b) rhombohedral ZrNCl, and (c) of hexagonal HfNCl showing bands in a window around the Fermi energy.

Interestingly, despite the highly layered nature of the title compounds, there is some dispersion along the directions perpendicular to the layers. An examination of suitable 'fat-bands' (where bands are decorated with the orbital character) shows that this dispersion arises due to the double-layered nature of the individual slabs and a weak Cl–Cl interaction across the van der Waals gap. It is seen that the compounds possess an indirect band gap between Γ and 0.2 in the Γ–M to the K point in the case of the hexagonal compounds. The dispersion of the different conduction bands allows us to recognize distinct saddle points in the hexagonal band structures at the M points. In the rhombohedral compound, the saddle points are not seen as clearly because the minima at K and H in the hexagonal band structures are no longer present.

Even at the level of the conduction band structure, clear differences between ZrNCl and HfNCl manifest that will become apparent when we examine the energy isosurfaces of the 'doped' compounds. At the energy where we find the instability at the *M* points in the two hexagonal band structures, namely at 3.5 eV for ZrNCl and 3.7 eV for HfNCl, there are three bands in the case of the former but only one in the case of HfNCl. This is because the band that is metal–metal bonding in the plane (with $d_{x^2-y^2}$ and d_{xy} character) is destabilized at the Γ point in the Hf compound compared with the Zr compound.

Within the van Hove scenario[2,3] we expect that these instabilities at the M point are implicated in the superconductivity. The optimally doped superconducting compounds would then correspond to compositions that have these instabilities at the Fermi level. We therefore consider the Fermi surfaces of the superconducting compositions by considering the isosurfaces of constant energy E_{SP} where E_{SP} are the energies (3.5 eV for ZrNCl and 3.7 eV for HfNCl) at which the saddle points at the M points are found. To determine the number of electrons that would need to be doped within a rigid band model in order that E_F is brought into coincidence with these E_{SP}, we integrate the total DOS from the E_F to E_{SP}. We find that in the case of ZrNCl, about 0.55 electrons per formula unit are required to bring about such coincidence. For HfNCl, the number is 0.39 electrons per formula unit. In other words, the highest T_c values should be found for the compositions $Li_{0.55}ZrNCl$ and $Li_{0.39}HfNCl$. It is interesting that while in HfNCl, the separation between E_{SP} and E_F is larger than for ZrNCl, in terms of the level of optimal doping (required to bring about the coincidence of E_{SP} and E_F) the saddle point is more accessible in HfNCl which indeed is the system that yields the superconductor with the higher T_c. The reason is that the additional electrons from the dopant atom go solely into the conduction band that forms the saddle point in the case of the Hf compound. In ZrNCl they go into two other bands as well.

Fig. 6 displays the surfaces of constant energy E_{SP} for (a) hexagonal ZrNCl and (b) hexagonal HfNCl. These would correspond within the rigid band model to the Fermi surfaces of $Li_{0.55}ZrNCl$ and $Li_{0.39}HfNCl$ respectively. The surfaces are decorated with the Fermi velocities with 'hotter' colours (yellow, orange, red) corresponding to regions of high Fermi velocity and the 'colder' colours (green, blue) corresponding to regions of low Fermi velocity. As seen in the band structure, in ZrNCl, since there are three bands at E_{SP}, the isosurface has three envelopes, while in HfNCl, there is only one band and correspondingly, only one envelope. In neither isosurface is there any structure along the Γ–A direction in keeping with

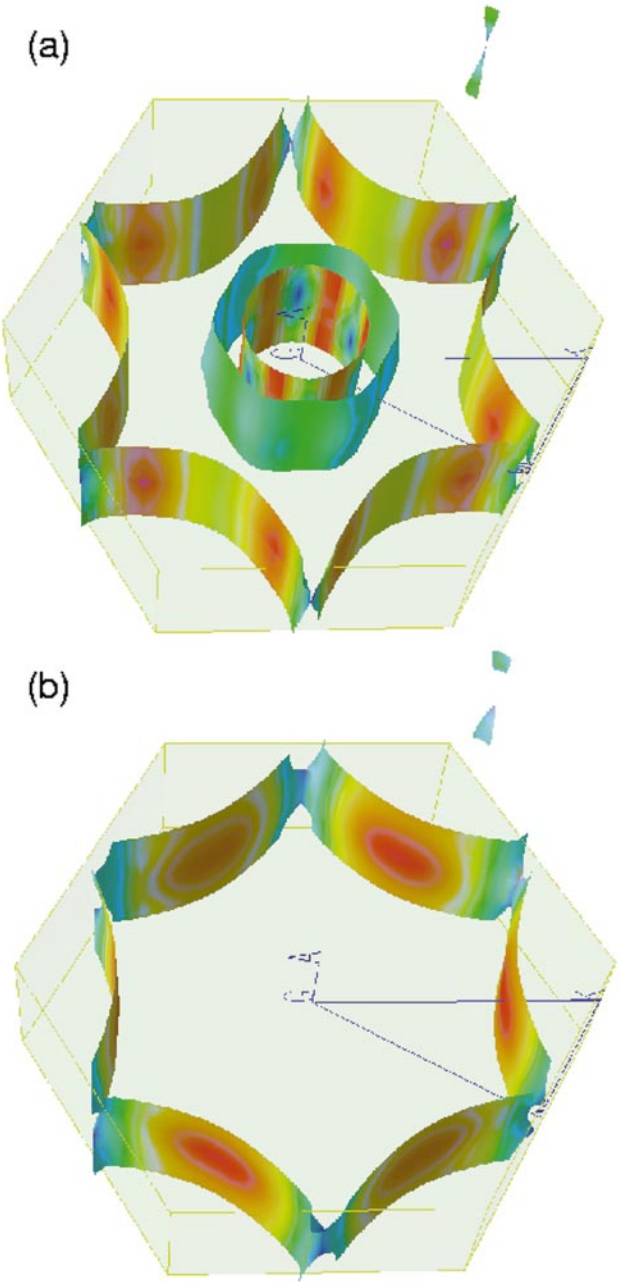

Fig. 6 Calculated energy isosurfaces corresponding to the positions of the saddle points in the conduction band of (a) hexagonal ZrNCl and (b) hexagonal HfNCl.

our expectation that these compounds are highly two-dimensional. In ZrNCl there are two concentric cylinders centered around Γ–A enclosing electrons. The third envelope has a shape that is somewhere between a six-pointed star and a hexagon, as in many layered d^1 hexagonal compounds.[15] In the region between the outer cylinder and the star, the carriers have hole character. The carriers outside this surface are electrons. It is this outer envelope that is important from the viewpoint of the transport properties.

We see that at the corners of the star namely the M point of the BZ the envelope is blue corresponding to regions of very low Fermi velocities. Looking from above, we observe that these blue regions have an X shape. Between these regions of low Fermi velocity are regions that are orange in colour corresponding to high Fermi velocities. This is similarly seen in HfNCl, where the single envelope also has a shape between a six-pointed star and hexagon but is closer to the latter. This isosurface simultaneously displays stronger nesting (more blue at the X point) and greater dispersion along the Γ–K line (more red). The greater dispersion along Γ–K in the Hf compound compared to the Zr compound is because the conduction band of the former is significantly raised in energy at the Γ point.

Discussion

The nature of the isosurfaces of the doped compounds seems familiar from discussions of the Fermi surfaces of other layered superconducting compounds.[6] In the next figure (Fig. 7) we compare schematically the Fermi surfaces of the cuprate superconductors (for example of hole-doped La_2CuO_4) with those of the title compounds projected in the plane reciprocal to the layers in the crystal structures. Both these Fermi surfaces share an important common feature namely a region of low Fermi velocity (a nested region) with a characteristic X shape.

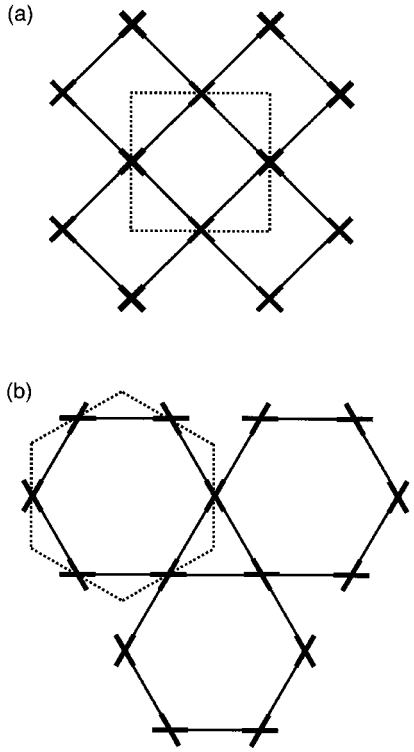

Fig. 7 Scheme of the Fermi surfaces of (a) the cuprate superconductors and (b) the title compounds projected on a plane. The dotted square and hexagon represent the respective BZs, the lines the FS and the Xs, regions of low Fermi velocity in the FS. Between the Xs are regions of high Fermi velocity.

While the carriers in the d^9 cuprates have hole character, the title compounds after doping (near d^1) have electrons as the charge carriers. What seems to be important for superconductivity is not only the nesting but also the simultaneous presence of highly disperse regions in the Fermi surface. In the two compounds examined here, the one with the higher T_c namely β-HfNCl does indeed have both these features expressed more strongly. Since it has only one band at the energy corresponding to the saddle point, the electron doping within our rigid band model also seems to be more efficient in HfNCl.

On the one hand, the layered cuprates have square-net topologies (allowing the 180° Cu–O–Cu superexchange interaction) a near d^9 electron count and no metal–metal bonding. On the other hand, the title compounds possess close to d^1 electron counts (when doped) metal–metal as well as metal–non-metal interactions and atom topologies that are completely different from those in the cuprates. It is interesting that despite these differences those aspects of the Fermi surfaces that we believe important for superconductivity seem to be features shared by both classes of compounds. The finding of the rather high T_c of 26 K in the β-HfNCl we believe provides the imperative to carefully examine the electronic structures of compounds showing patterns of instabilities that seem increasingly implicated in superconductivity.

Acknowledgements

Professor O. K. Andersen and Dr. O. Jepsen are thanked for providing the LMTO codes and for encouragement, and Professor W. Tremel and Dr. J. Neuhausen for useful discussions. We are grateful to Dr. Hj. Mattausch for information on the structure of ZrNCl. Financial support from the German Fonds der chemischen Industrie is acknowledged.

References

1 J. Labbé and J. Friedel, *J. Phys. (Paris)*, 1966, **27**, 153.
2 J. Labbé and J. Bok, *Europhys. Lett.*, 1987, **3**, 1225.
3 D. M. Newns, H. R. Krishnamurthy, P. C. Pattnaik, C. C. Tsuei and C. C. Chi, *Physica B*, 1993, **186**, 801.
4 C. Felser, *J. Alloys Compd.*, 1997, **61**, 87.
5 C. Felser, S. Cramm, D. Johrendt, A. Mewis, O. Jepsen, G. Hohlneicher, W. Eberhardt and O. K. Andersen, *Europhys. Lett.*, 1997, **40**, 85.
6 C. Felser, R. Seshadri, A. Leist and W. Tremel, *J. Mater. Chem.*, 1998, **8**, 787.
7 C. Felser, P. Deniard, M. Bäcker, T. Ohm, J. Rouxel and A. Simon, *J. Mater. Chem.*, 1998, **8**, 1295.
8 M. J. Geselbracht, T. J. Richardson and A. M. Stacey, *Nature*, 1990, **345**, 6273.
9 D. L. Novikov, V. A. Gubanov and V. G. Zubkov, *Phys. Rev. B*, 1994, **49**, 15830.
10 R. Seshadri, C. Felser, K. Thieme and W. Tremel, *Chem. Mater.*, 1998, **10**, 2189.
11 S. Yamanaka, H. Kawaji, K. Hotehama and M. Ohashi, *Adv. Mater.*, 1996, **9**, 771.
12 H. Kawaji, K. Hotehama and S. Yamanaka, *Chem. Mater.*, 1997, **9**, 2127.
13 S. Yamanaka, K. Hotehama and H. Kawaji, *Nature*, 1998, **392**, 580.
14 O. Jepsen and O. K. Andersen, *Z. Phys. B*, 1995, **97**, 35.
15 C. Felser, K. Thieme and R. Seshadri, *J. Mater. Chem.*, in press.
16 P. M. Woodward and T. Vogt, *J. Solid State Chem.*, 1998, **138**, 207.
17 R. Juza and H. Friedrichsen, *Z. Anorg. Allg. Chem.*, 1966, **622**, 123.
18 F. Lissner and T. Schleid, Poster presented at the DFG Solid State Chemistry Symposium, Saarbrücken, Germany, 1998.
19 H.L. Skriver, *The LMTO method*, Springer, Berlin, 1984.
20 O. K. Andersen, O. Jepsen *et al.*, The Stuttgart TB-LMTO-ASA

Program version 47, MPI für Festkörperforschung, Stuttgart, Germany, 1996.
21 C. J. Bradley and A. P. Cracknell, *The mathematical theory of symmetry in solids*, Clarendon Press, Oxford, 1972.
22 F. Boucher, O. Jepsen and O. K. Andersen, unpublished results.
23 S. Wijeyesekera and R. Hoffmann, *Organometallics*, 1984, **3**, 949.
24 A. Simon, A. Yoshiasa, M. Bäcker, R.W. Henn, C. Felser, R. K. Kremer and Hj. Mattausch, *Z. Anorg. Allg. Chem.*, 1996, **622**, 123.
25 Y. Tian and T. Hughbanks, *Inorg. Chem.*, 1993, **32**, 400; K. A. Yee and T. Hughbanks, *Inorg. Chem.*, 1991, **30**, 2321.

Paper 8/08127A